

# Mechanical Design and Drafting of the FRS Ion Catcher Radiation Shielding

Facility for Antiproton and Ion Research in Europe and  
GSI Helmholtzzentrum für Schwerionenforschung

GASPER BIZJAN



Internship and Training Project Report  
Darmstadt, Germany  
31-01-2024

GET INVOLVED 2023: GI-231656B-SL-SIE



**Copyrights(c)**

Personal use of this material is permitted. However, permission to reprint/republish this material for advertising or promotional purposes or for creating new collective works for resale or redistribution to servers or lists, or to reuse any copyrighted component of this work in other works must be obtained from the GSI GmbH and FAIR GmbH.

**Author(s)**

Gasper Bizjan

University of Ljubljana, Faculty of Mechanical Engineering

Aškerčeva 6, 1000 Ljubljana, Slovenia

Email: gasper212.bizjan@gmail.com

**Project Mentor/Supervisor**

Dr. Timo Dickel/Supervisor name

FRS/SFRS

GSI Helmholtzzentrum für Schwerionenforschung GmbH,

Planckstr. 1, 64291 Darmstadt, Germany

Tel: +49 6159 71 2733

Email: T.Dickel@gsi.de

**Program Coordinator**

Dr. Pradeep Ghosh

GSI Helmholtzzentrum für Schwerionenforschung GmbH &

Facility for Antiproton and Ion Research in Europe GmbH

Tel: +49 6159 71 3257, Fax: +49 6159 71 3916

Email: Pradeep.Ghosh@fair-center.eu

**GET Involved 2023: GI-231656B-SL-SIE**

Publisher: GSI Helmholtzzentrum für Schwerionenforschung GmbH,  
Planckstr. 1, 64291 Darmstadt, Germany

Published: February 2024



# Abstract

In this report, we will discuss the results and the process of the full-time internship on the 'Mechanical Design and Drafting of the FRS Ion Catcher Radiation Shielding', as part of the Thermalized exotic nuclei group in the FRS/SFRS experiments department at GSI. The team at the FRS has an incorporated research project with the IAEA on fission yields of actinides. They study this by measuring the products from spontaneous fission sources by high-resolution mass spectrometry. To increase the sensitivity of the method they aim to use stronger radioactive sources. For these an upgraded radiation safety concept has already been developed and simulated. Now the design and drafting of the mechanical parts is the next step needed for the realization of the project. The work started with studying the developed radiation safety design, after that, a 3D CAD model was done and iterated upon with the group (incl. engineers). Once the final design was selected and confirmed (both from the team at GSI as well as the manufacturers), the final technical documentation was drafted so the parts could be ordered and produced. Apart from the radiation shielding, the internship also included minor projects, such as designing the glovebox.



## **Declaration**

I hereby declare that the project entitled '**Mechanical Design and Drafting of the FRS Ion Catcher Radiation Shielding**' is my own work and that I have correctly acknowledged the work of others.



## Acknowledgements

I would like to thank the FRS/SFRS team at GSI for guiding me through the process of developing the radiation shielding solution for the Ion Catcher. The teamwork and mentorship quality exhibited was of the highest caliber. I would especially like to thank my mentor Dr. Timo Dickel for moving the project forward when it appeared stuck, my direct supervisor Dr. Daler Amanbayev for always being available to answer questions and also Michael Will for guiding me with official GSI business. A warm thanks to Dr. Pradeep Ghost and the team in the International office, who gave me the chance to be a part of the Get Involved 2023 project.



# Contents

<b>Contents</b> . . . . .	vii
<b>List of Figures</b> . . . . .	ix
<b>List of Tables</b> . . . . .	x
<b>1 Introduction</b> . . . . .	1
1.1 Independent isotopic fission yields of spontaneous fission via mass measurements at the FRS IC . . . . .	1
1.2 The goal of the Internship project . . . . .	3
<b>2 FRS Ion Catcher</b> . . . . .	4
2.1 Cryogenic gas-filled Stopping Cell . . . . .	6
<b>3 Requirements and specifications</b> . . . . .	7
<b>4 Modeling and simulations</b> . . . . .	10
4.1 Comparing the 3D model to the physical system . . . . .	10
4.2 Technical models . . . . .	10
4.2.1 Radiation dose analysis . . . . .	10
4.2.2 Structural analysis . . . . .	11
4.2.2.1 Structural analysis of the shielding . . . . .	12
4.2.2.2 Structural analysis of supporting bars . . . . .	13
4.2.2.3 Structural analysis of the frame . . . . .	15
4.3 Cost model . . . . .	17
<b>5 Engineering Standards</b> . . . . .	18
5.1 Radiation standards . . . . .	18
5.1.1 Ionizing radiation . . . . .	18
5.1.2 Neutron shielding properties . . . . .	19
5.1.3 Radiation shielding design principles . . . . .	20
5.2 Fire safety standards . . . . .	21
5.2.1 Conditions of operation of the CSC experiment . . . . .	21
5.2.2 Fire classification of construction products and elements . . . . .	21
5.2.3 UL94 V Flammability Standard . . . . .	24
<b>6 Material and company selection</b> . . . . .	25
6.1 The selection process . . . . .	25
6.2 Companies contacted for fire-resistant HDPE . . . . .	26

6.2.1	Röchling Group . . . . .	26
6.2.2	JCS Nuclear Solutions . . . . .	26
6.2.3	Mitsubishi Chemical Group . . . . .	27
6.2.3.1	The change in radiation dose . . . . .	28
<b>7</b>	<b>Design process . . . . .</b>	<b>29</b>
7.1	Mechanical solution conceptualisation . . . . .	29
7.2	The iterative process and the final design . . . . .	30
7.3	Technical documentation . . . . .	31
<b>8</b>	<b>Conclusion . . . . .</b>	<b>32</b>
<b>9</b>	<b>Bibliography . . . . .</b>	<b>33</b>
<b>10</b>	<b>Appendix . . . . .</b>	<b>34</b>

# List of Figures

1.1	Cross section of the CSC with the internal long DC cage that is optimized for thermalizing relativistic ions. The $^{252}\text{Cf}$ SF source is installed 9 cm off-axis. The red lines mark the approximate range of the emitted FPs [1]. . . . .	2
1.2	<i>Geant4</i> simulation results of a 10 Mbq $^{252}\text{Cf}$ source. . . . .	3
1.3	(a) The CSC and (b) the initial CAD of the shielding. . . . .	3
2.1	Schematic view of the setup of the FRS Ion Catcher, including the stopping cell, the RFQ beam line and the MR-TOF-MS [2]. . . . .	5
2.2	Physical CSC as found in the S4 cave at GSI Experimental Hall. . . . .	6
4.1	Schematic view of ANSYS simulation set-up. . . . .	11
4.2	The deformation and tilting FEM results of the shielding. . . . .	12
4.3	The reaction forces FEM results of the shielding. . . . .	13
4.4	The reaction forces FEM results of the shielding. . . . .	14
4.5	The von-Misses stress FEM results of brown bar at $F_{\max}$ . . . . .	14
4.6	Total deformation in the frame and the forces involved. . . . .	15
4.7	Maximum (top) and minimum (bottom) combined stress of the frame. . . . .	16
5.1	Table of properties of HDPE [3]. . . . .	19
5.2	Example of a three-chevron brick [4]. . . . .	20
5.3	General diagram of a chevron block assembly [4]. . . . .	20
5.4	Fire test according to ISO 13501-1 [5] . . . . .	22
5.5	UL94 burning test [7]. . . . .	24
6.1	Chevron design changed by Mitsubishi. . . . .	27
7.1	Concept sketching for the stopping cell shielding. . . . .	29
7.2	Full shielding solution from the front (left) and the rear (right). . . . .	30
7.3	Installed glovebox within the shielding. . . . .	30
7.4	Exploded view of the shielding. . . . .	31

# List of Tables

3.1	All the project's needs categorised and numbered by importance. . . . .	8
3.2	Specification of the CSC neutron shielding. . . . .	9

# 1 Introduction

GSI Helmholtzzentrum für Schwerionenforschunghe in Darmstadt operates a worldwide leading accelerator facility for research purposes. Experiments using highly radioactive sources are performed at the Fragment separator (FRS), which raises the need for highly specialised radiation shielding. In the following report the design process of such a shielding is discussed.

## 1.1 Independent isotopic fission yields of spontaneous fission via mass measurements at the FRS IC

First we will have an overview of the experiment that has a need for radioactive sources. The nuclear fission process has wide basic and applied scientific implications, including nuclear structure and reactions and the abundance of elements through nucleosynthesis, nuclear waste management and radiation safety.

In the context of nuclear physics, Independent Isotopic Fission Yields (IIFYs) are measurements that detail the individual yields of different isotopes produced as a result of a fission event. In a fission event, a heavy nucleus splits into two or more smaller nuclei along with the emission of neutrons and gamma rays. The specific isotopes that are produced in this process, and their respective quantities, are what constitute the fission yields. IIFYs provide access to the probability distribution of fission products, which contribute to understanding nuclear fission in more depth than mass yield distributions. Measurements of SF properties are important for the basic understanding of fission since the fission process takes place at a specific excitation energy, which enables researchers to benchmark theories. This method can also be applied for neutron-induced fission at various incoming neutron energies [1].

The International Atomic Energy Agency (IAEA) recommended to pursue fission yield measurements via direct ion counting. This method was utilised at GSI using the Fragment Separator Ion Catcher (FRS-IC), by Utilizing its high-resolving multiple-reflection time-of-flight mass-spectrometer (MR-TOF-MS).

A  $^{252}\text{Cf}$  SF source with an activity of 20 kBq is installed inside a cryogenic stopping cell (CSC), where the fission products (FPs) are thermalized in the CSC buffer gas and are then extracted, diagnosed and transported by a versatile RFQ beam-line (Fig. 1.1). They are identified via accurate mass measurement by a MR-TOF-MS, which can separate isobars and thus provide unambiguous identification of the FPs.

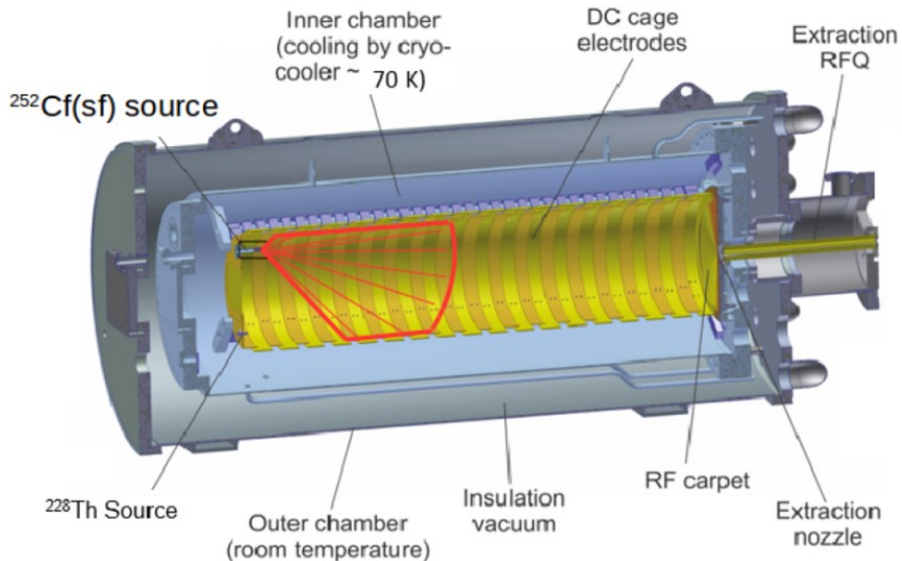


Figure 1.1: Cross section of the CSC with the internal long DC cage that is optimized for thermalizing relativistic ions. The  $^{252}\text{Cf}$  SF source is installed 9 cm off-axis. The red lines mark the approximate range of the emitted FPs [1].

Future measurements require the use of higher radioactive sources, specifically a  $^{252}\text{Cf}$  source with higher activity, for two primary reasons:

- **Increased Efficiency:** The use of a higher activity source is expected to significantly improve the stopping and extraction efficiency of fission products. This efficiency enhancement is projected to be at least an order of magnitude higher than current levels.
- **Enabling Systematic Comparisons and Access to Lower Fission Yields:** A higher activity source will allow for the investigation of lower fission yields. That will enable systematic comparisons of different fissioning systems, which is crucial for a deeper understanding of the fission process and its various outcomes.

Therefore the plan is to implement a 10 MBq  $^{252}\text{Cf}$  source. Such a radioactive source raises the need for extra radiation shielding.

## 1.2 The goal of the Internship project

With the need for radiations shielding an initial design was presented at the beginning of the internship. The safety threshold was set to  $0.5 \mu\text{Sv}/\text{h}$ . The material and thickness of the shielding were determined using the results of the simulation software *Geant4* for the passage of particles through matter. The particles were selected to be neutrons, therefore the radiation shielding is technically neutron shielding. As will be explained in a later chapter, one of the options for neutron shielding is polyethylene, which was also the material used in the simulation (Fig. 1.2).

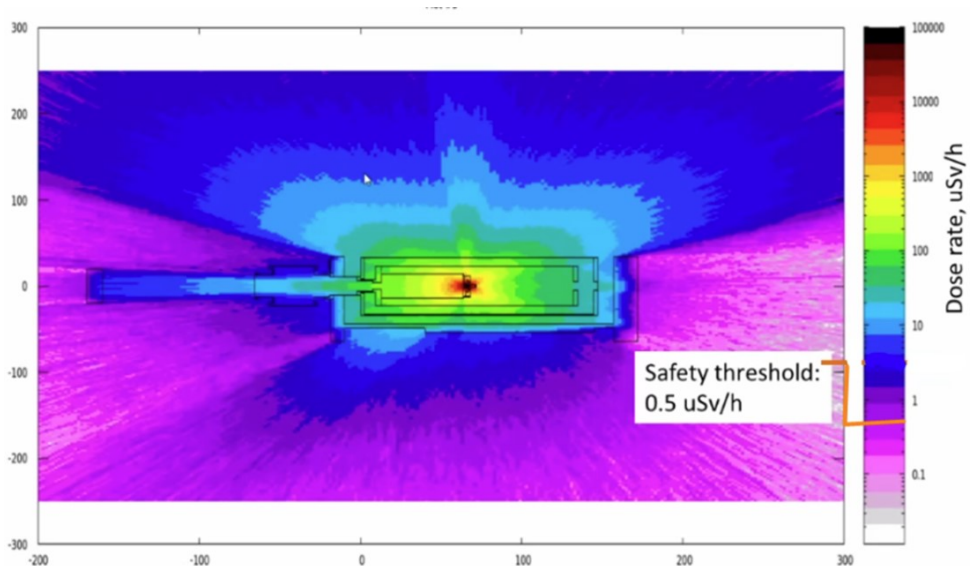


Figure 1.2: *Geant4* simulation results of a 10 Mbq  $^{252}\text{Cf}$  source.

A basic model of the shielding (Fig. 1.3b) was designed around the CSC (Fig. 1.3a) of the FRS-IC, using the CAD software *CATIA*. Based on the simulation results and the initial design, a full mechanical solution is to be implemented.

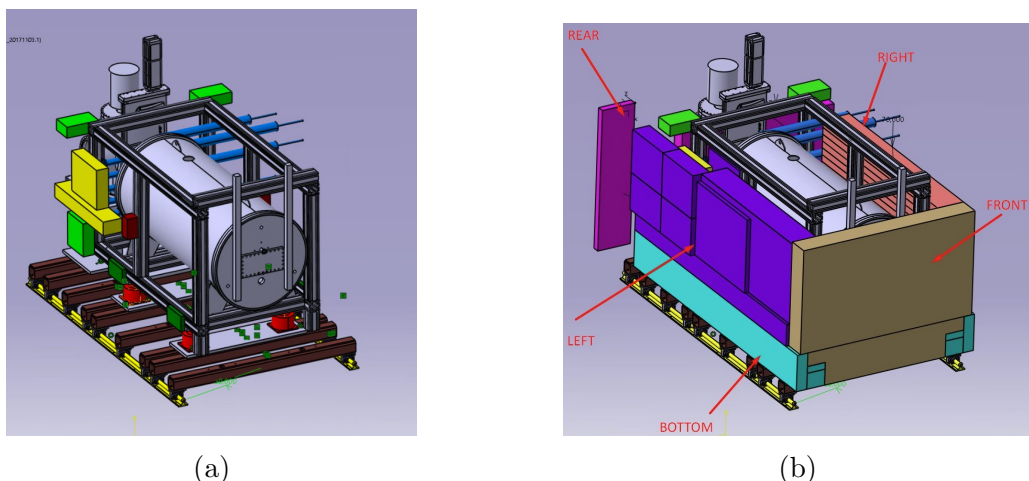


Figure 1.3: (a) The CSC and (b) the initial CAD of the shielding.

## 2 FRS Ion Catcher

Let's begin by understanding the system of interest - the FRS (FRagment Separator) Ion Catcher (IC) (Fig. 2.1). The FRS-IC is an ion-optical device used to focus and separate products from the collision of relativistic ion beams with thin targets [2].

At GSI, projectile and fission fragments are produced at relativistic energies, separated in-flight, range-focused, slowed down and thermalized in a cryogenic stopping cell. A multiple-reflection time-of-flight mass spectrometer (MR-TOF-MS) is used to perform direct mass measurements and to provide an isobarically clean beam for further experiments, such as mass-selected decay spectroscopy. A versatile RF quadrupole transport and diagnostics unit guides the ions from the stopping cell to the MR-TOF-MS, provides differential pumping, ion identification and includes reference ion sources.

The FRS Ion Catcher serves as a test facility for the Low-Energy Branch of the Super-FRS at the Facility for Antiproton and Ion Research (FAIR), where the cryogenic stopping cell and the MR-TOF-MS will be key devices for the research of:

- direct mass measurements of neutron-deficient nuclides,
- measurement of  $\beta$ -delayed neutron emission probabilities and
- independent isotopic fission yields of spontaneous fission (IIFY of SF).

The FRS Ion Catcher consists of four main parts:

- the FRS including a monoenergetic degrader system,
- Cryogenic gas-filled Stopping Cell (CSC),
- RF-quadrupole-based beam transport and diagnostics unit and
- the multiple-reflection time-of-flight mass spectrometer.

The main subsystem of interest will be the CSC and we will take a closer look at it.

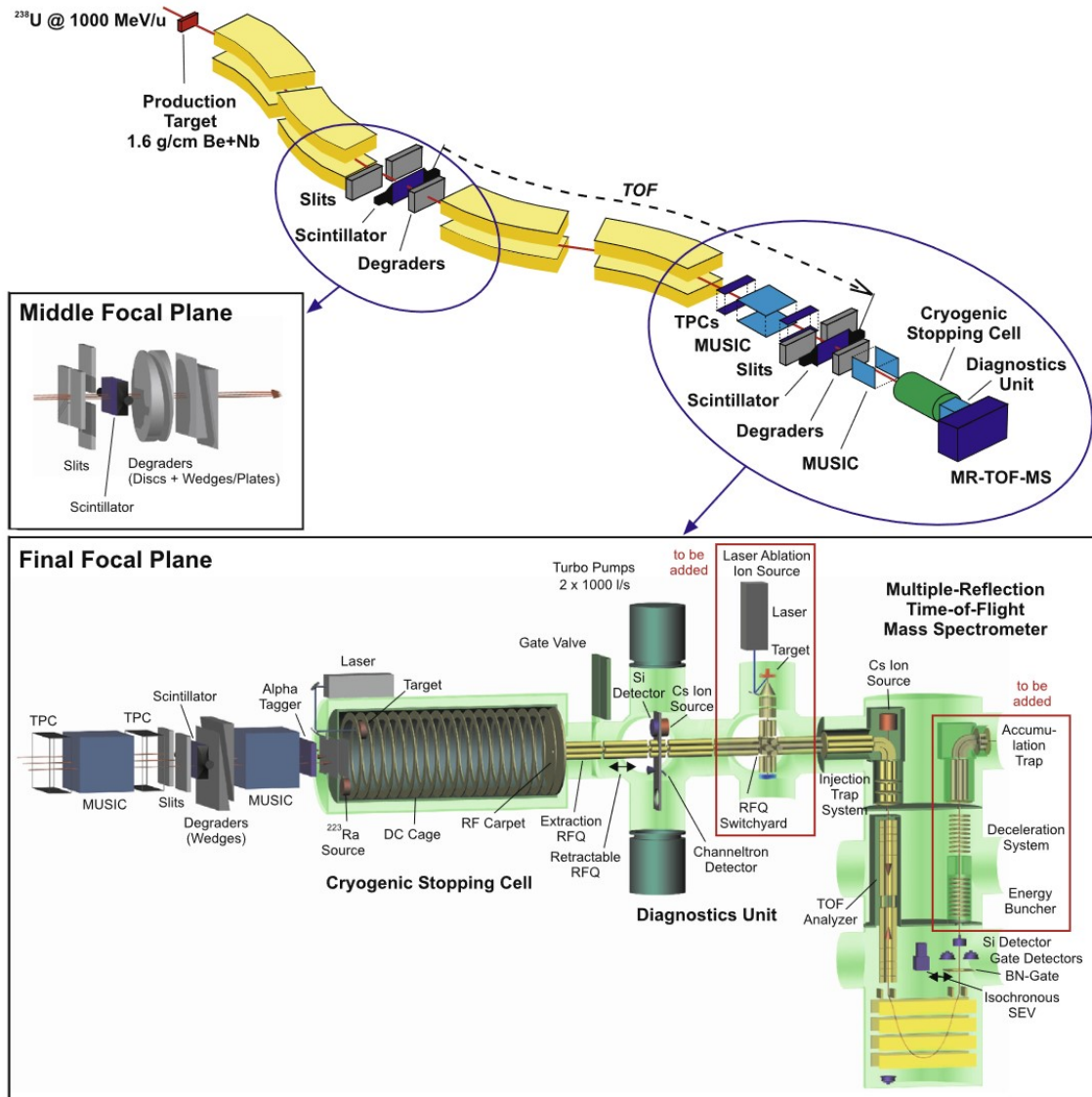


Figure 2.1: Schematic view of the setup of the FRS Ion Catcher, including the stopping cell, the RFQ beam line and the MR-TOF-MS [2].

## 2.1 Cryogenic gas-filled Stopping Cell

Efficient stopping of range-bunched beams from the FRS requires a stopping gas with an areal density from about 2–20 mg/cm<sup>2</sup>, depending on reaction type and primary beam energy. An area 10 cm high and 25 cm wide should be covered to accommodate the cross-sectional area of the beam. Following these requirements, a cryogenic stopping cell (Fig. 2.2) with a stopping volume with a length of 105 cm and a diameter 25 cm has been designed and built. It uses helium as stopping gas. An outer chamber with a length of 145 cm and a diameter of 66 cm provides the insulation vacuum for the inner cryogenic chamber.

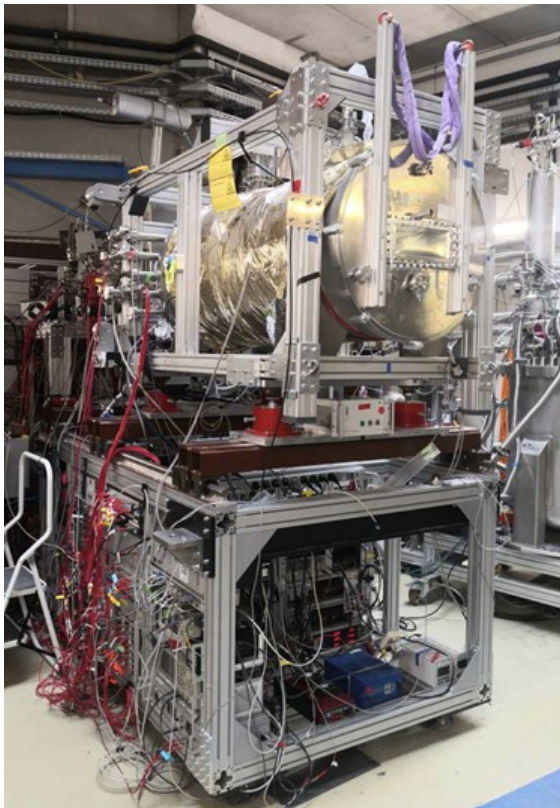


Figure 2.2: Physical CSC as found in the S4 cave at GSI Experimental Hall.

During beam-time, ions enter the stopping cell through two stainless steel windows with a thickness of 100  $\mu\text{m}$ . A DC field created by a DC cage with ring electrodes throughout the length of the cell drags the ions towards the exit side of the stopping cell. There, an RF carpet with a ring electrode density of 4 electrodes/mm creates a repulsive RF field with a focusing DC field superimposed to guide the ions radially towards the exit-hole. Once the ions reach the exit, the gas flow drags them from the CSC.

The experiment requiring the shielding, is done during offline times. Then, the CSC is equipped with a internal source and a laser ablation ion source mounted at the entrance of the inner chamber of the cell. These sources provide ions for tests, performance measurements and for calibration of accurate mass measurements with the MR-TOF-MS, but are a source of significant ionizing radiation.

## 3 Requirements and specifications

The first step is to identify the requirements of the shielding, which stem from the needs of the team using the CSC and the experiment. The process of identifying the needs is an integral part of the larger product development process and is most closely related to concept generation, concept selection, the establishment of project specifications and iterative design change.

Based on the problem definition, the existing simulated design (Fig. 1.3a) and speaking with the team the following needs need to be met:

- Safety radiation dose is  $1000 \mu\text{Sv}/\text{year}$ . For someone working 8 h/day that is:

$$\frac{1000 \mu\text{Sv}/\text{year}}{8 \text{ h/day} \times 260 \text{ day/year}} \approx 0.5 \mu\text{Sv/h}$$

- The design of the original Ion catcher stays the same! Shielding is added without changing what is already there. The assembly process of the CSC must be taken into account.
- The material used is polyethylene / borated polyethylene.
- Shielding should be fire resistant as per GSI standards (P10 gas is used in the experiment cave).
- Total weight approx. 1.35 tons.
- Design is split into 5 parts: bottom, left, right, front, rear.
- Preliminary design of the shielding, should be followed as closely as possible (minimal material extrusion, if material is extruded, then it should be added, etc.).
- A glovebox is planned to be used during the transport and insertion of the fission source.

The simple statements above can be further organised into categories, from which more detailed and tangible needs can be established. We will also set the relative importance of different needs. A sense of the relative importance of the various needs is essential to making trade-offs in the design process correctly. We will give every detailed need in table 3.1 an importance from 1 to 5 - 1 being the least important and 5 the most important need.

A need of value of 1 can even be omitted if necessary, while one with 5 is non-negotiable. The importance of the needs can still be iteratively changed during the later step of setting final specifications.

Table 3.1: All the project's needs categorised and numbered by importance.

No.	Category	Need	Imp.
1	Safety	in terms of radiation exposure.	5
2	Safety	in terms of fire resistance.	5
3	Design	should not change the current CSC at all.	4
4	Assembly	must be easy to do, as well as disassembly.	3
5	Assembly	is supported only from below (frame).	4
6	Materials	are available at GSI.	1
7	Assembly	by hand around important parts for accessibility.	2
8	Assembly	of heavy parts is done with crane.	3
9	Design	follows preliminary simulation.	3
10	Design	has 5 parts - bottom, front, rear, left, right.	1
11	Design	accounts for S4 cave size.	5
12	Materials	are polyethylene and borated polyethylene.	2
13	Made	by GSI workshop	1
14	Price	has to be kept low.	3
15	Design	has to account for the glovebox .	3
16	Design	has to account for transport box.	4
17	Design	has to make sure the frame is strong enough.	5
18	Materials	are manufacturable.	5

While such expression of needs is helpful in developing a clear sense of the issues of interest, they provide little specific guidance about how to design and engineer the shielding. They simply leave too much margin for subjective interpretation. For this reason, we established a set of specifications, which spell out in precise, measurable detail what the shielding has to do and the qualities it must have.

A specification consists of a metric and a value. A metric is a quantifiable representation of a need - a unit of measurement. We can see the specification of the CSC neutron shielding, from which the design process will come from, in table 3.2. The importance is still there like before, but we added measurable metrics (units), with an ideal selected value, as well as an acceptable range that can be used during the trade-off process.

With the specification known and set, we will now develop a few models of the project, that will predict the approximate technical design, as well as the cost. Some of the specification require basic calculation and simulations.

Table 3.2: Specification of the CSC neutron shielding.

No.	Need Nos.	Metric	Imp.	Units	Sel. val.	Min. val.	Max. val.
1	1	Dose rate	5	microSv/h	0.5	0	0.5
2	3, 6, 9	Number of changes to current CSC setup	4	Count	0	0	15
3	4	People needed for assembly process	1	Count	1-2	2	4
4	4, 7, 8, 10	assembly time	2	h	8	1	16
5	4, 8	Number of crane lifts	1	Count	0	2	15
6	4, 8	Heaviest part for crane lifting	3	kg	0	x	2000
7	4, 7	Heaviest part for lifting by hand (per person)	4	kg	30	x	40
8	2, 12	GSI fire-safety instructions for material used	5	LOI	x	x	x
9	2, 12	Amount of flammable material	5	kg	x	x	x
10	6	Amount of material already at GSI	2	% of tot.	0	0	100
11	11	Length of the shielding	4	mm	2541	2472	2472
12	11	Width of the shielding	4	mm	1460	1362	1462
13	11	Height of the shielding	4	mm	1035	1035	1380
14	6, 14, 12	Price of project	3	EUR	18000	10000	30000
15	5, 12	Total new mass	2	kg	1600	1350	1800
16	7, 14	Manufacturing time	1	h	24	8	40
17	6, 14	Manufacturing processes	2	Count	2	1	3
18	4, 15	Time to install glovebox	2	h	0.5	1	1
19	4, 16	Time to insert transport box	2	h	0.5	1	1
20	8, 9, 10	Amount of original design kept	3	% of tot.	x	x	x
21	5	Compressive stress on red pillars	4	MPa	x	x	x
22	5, 14	Brown-bars needed	3	Count	9	6	9
23	5	Bars max. displacement	4	mm	0.2	0	1
24	5	Force on Brown-bar supports	4	N	2200	0	2500
25	17	Glove-box	3	Count	x	x	x
26	18	Thickness of the shielding plates	5	mm	50, 100	11.5	120
27	18	width of the plates	4	mm	x	x	2400
28	18	Length of the plates	4	mm	x	x	6000

# 4 Modeling and simulations

The difficult part of refining the specifications is choosing how such trade-offs will be resolved. For this we develop a technical model and a cost model. We can then refine some of the specifications using those models. The specifications seen above, are the final ones, gathered using the models shown below.

## 4.1 Comparing the 3D model to the physical system

Before we use the existing 3D CAD model of the CSC for any simulations, we have to check its accuracy around the most important parts. In the first part at the beginning of this internship, we did measurements of the stopping cell seen on figure 2.2 and compared it to the 3D model. We found some minor mismatches, which we fixed in the CAD model. With an accurate CAD of the CSC, we can proceed to the technical models.

## 4.2 Technical models

A technical model of the project is a tool for predicting the values of the metrics for a particular set of design decisions. Ideally, we will be able to accurately model the shielding analytically or with computer simulations. Such a modeling allows us to rapidly predict what type of performance can be expected from a particular choice of design variables, without costly physical experimentation.

### 4.2.1 Radiation dose analysis

Obviously the first technical model is the one already developed. The radiation simulation (Fig. 1.2) already determined the needed thicknesses and dimensions of the shielding, assuming High density polyethylene (HDPE), to achieve  $0.5 \mu\text{Sv}/\text{h}$ .

We notice the closer the shielding is to the source (in the centre of the CSC) the thicker it must be. The thickness of the shield can vary between 50 to 200 mm.

## 4.2.2 Structural analysis

Since the weight of the shielding is not insignificant, we need to do a structural analysis of the shielding and see the effects the added weight has on the bars and the frame. For the structural analysis we used the Finite Element Method (FEM) simulation software *ANSYS Mechanical* (Fig. 4.1).

The steps of the simulation are as follows:

**Step 1:** discretization of the physical model into Finite Elements (FE).

**Step 2:** selecting an approximation model.

**Step 3:** FE matrix formation.

**Step 4:** going from local FE matrix to a global system matrix.

**Step 5:** setting the boundary problem.

**Step 6:** solving the system of equations.

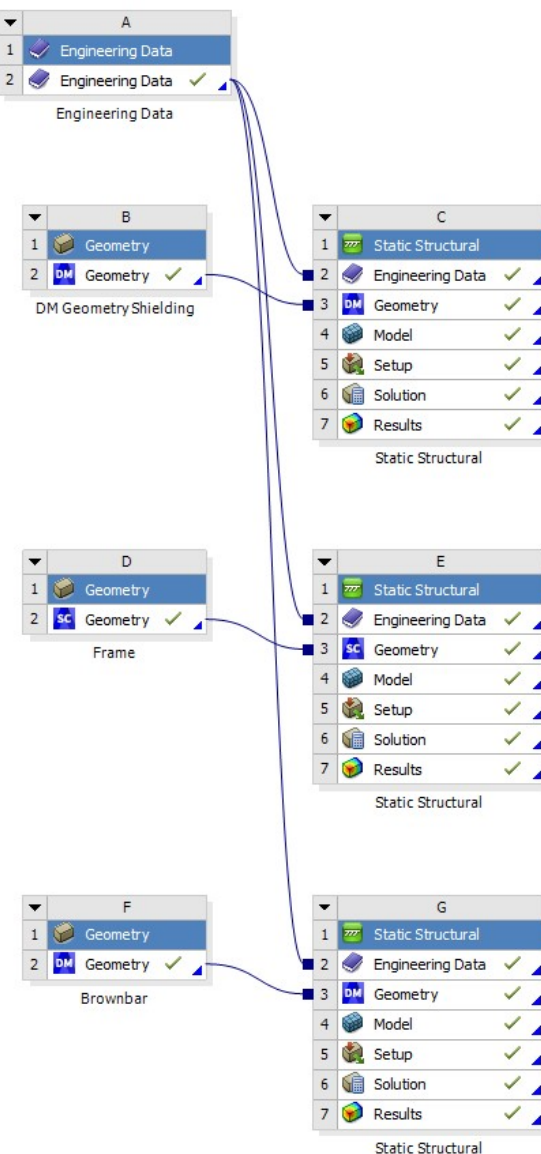


Figure 4.1: Schematic view of ANSYS simulation set-up.

#### 4.2.2.1 Structural analysis of the shielding

In order to see if the stresses within the shielding itself and to determine if there are any parts that need additional supports, a structural analysis of the shielding is needed. The simulation was done using the geometry from the initial 3D model, without the frame, the bars or the CSC. Slight modifications were made to reduce the unnecessary complexity of the model and allow better meshing.

For a static structural analysis, the material properties needed are primarily the density  $\rho$ , Young's modulus  $E$  and the Poisson ratio  $\nu$  of the materials used. After an initial research into HDPE (section 6), we assume an average representative of the material with  $\rho = 1030 \text{ kg/m}^3$ ,  $E = 1080 \text{ MPa}$  and  $\nu = 0.4$ . The supports included are made of structural steel with a  $\rho = 7850 \text{ kg/m}^3$ ,  $E = 200\,000 \text{ MPa}$  and  $\nu = 0.3$ .

The mesh is made out of 127131 hexagonal elements of type SOLID186 with 608295 nodes. SOLID186 is a full 3D FE type.

As seen below, the shielding is supported with fixed supports, where the brown bars are. It is also supported at the back, where the stopping cell and the MR-TOF are connected. The only force working on the shield is the resulting gravitational force with the constant  $g$ .

First let's have a look at the total deformation. We see that only the steel rear holders of the shielding are deformed to a noticeable degree (Fig. 4.2). With a thick enough plate for the holder, the deformation can be reduced further. The shielding itself has low internal stress and deformation.

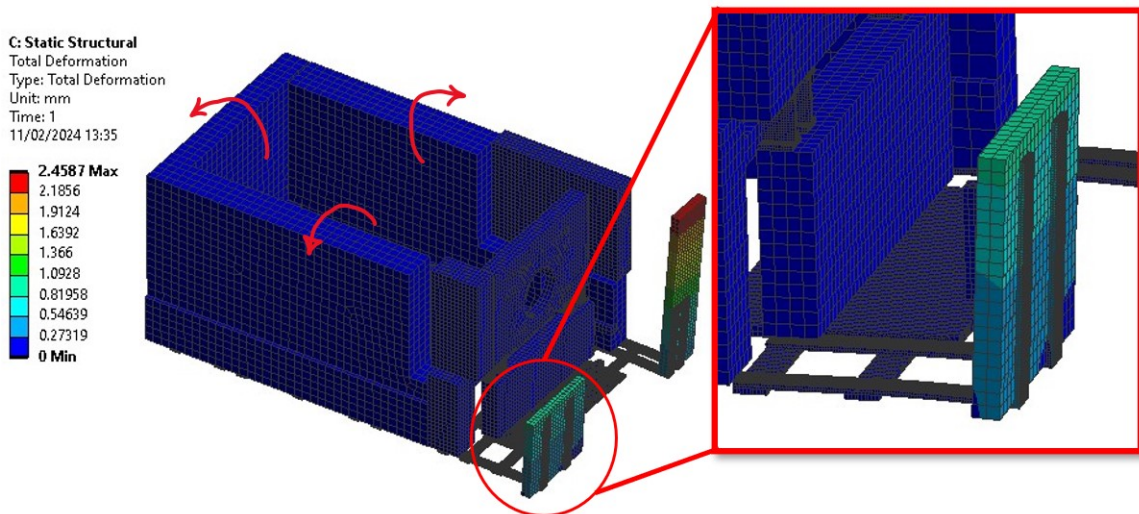


Figure 4.2: The deformation and tilting FEM results of the shielding.

The only issue becomes the stability of the shielding. As seen in the figure above, the shielding is not properly supported against tilting (red arrows). Extra supports at the front and the rear are to be implemented, that can keep the shielding together without the danger of it falling over.

#### 4.2.2.2 Structural analysis of supporting bars

In the previous simulation of the shielding we were able to acquire the resulting forces the brown bars must support (Fig. 4.3). We get the reaction forces  $F_1 = 3352$  N,  $F_2 = 4319$  N,  $F_3 = 3718$  N,  $F_4 = 1625$  N,  $F_5 = 3877$  N,  $F_6 = 4152$  N,  $F_7 = 833$  N,  $F_8 = 1170$  N,  $F_9 = 893$  N. The forces are assumed to be a purely vertical.

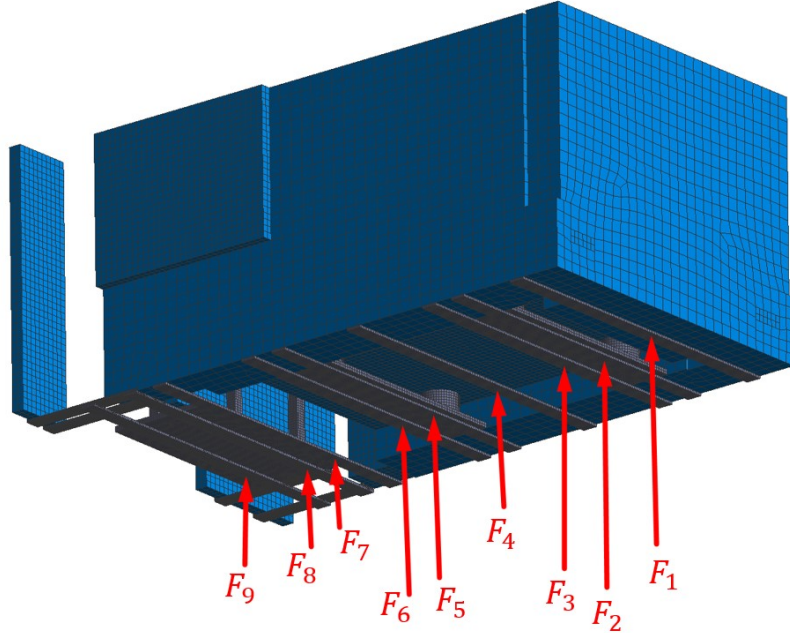


Figure 4.3: The reaction forces FEM results of the shielding.

If we take the maximum reaction force  $F_2$ , we can do a FEM analysis of the bars, by assuming the opposite and equal force acts on the brown bar. We already know the material of the brown bar (structural steel).

We only need to study half of the brown bar due to symmetry. One side has a symmetric boundary condition and the other has a joint condition. The element type is a combination of tetrahedral element SOLID187 and hexagonal SOLID186 with 228123 elements and 457340 nodes.

We see the total deformation is no more than 0.12 mm while using 9 brown bars (Fig. 4.4) and the maximum expected stress is no more than 74 MPa (Fig. 4.5), which is not close to the yield strength of  $\approx 300$  MPa.

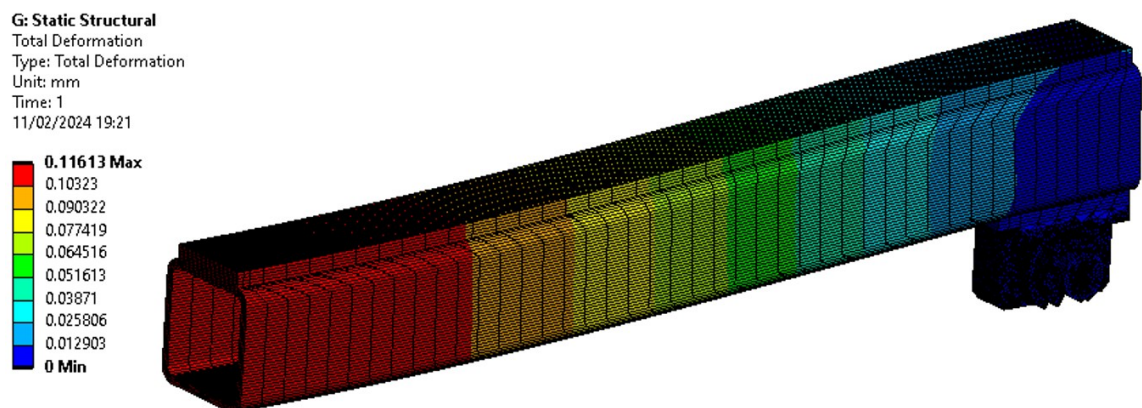


Figure 4.4: The reaction forces FEM results of the shielding.

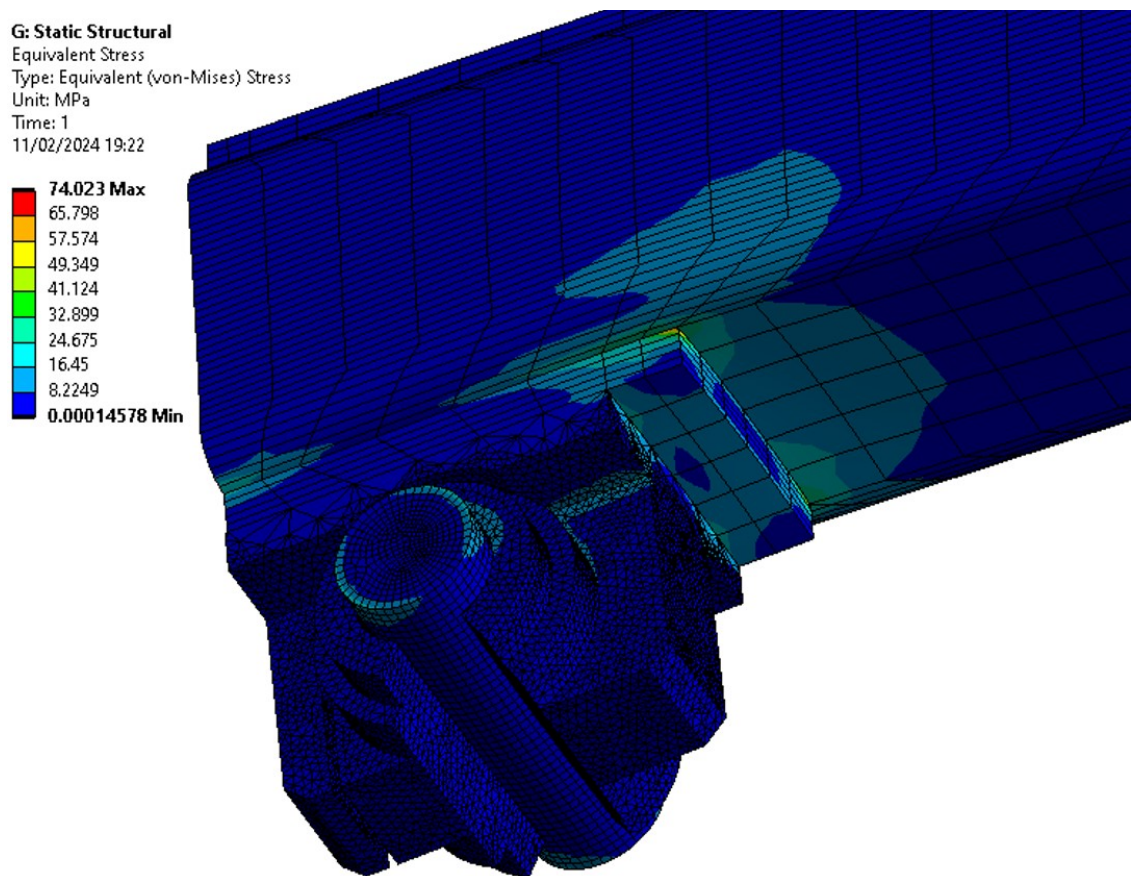


Figure 4.5: The von-Misses stress FEM results of brown bar at  $F_{\max}$ .

#### 4.2.2.3 Structural analysis of the frame

We also know the known reaction forces  $F_1$  to  $F_9$  are imposed on the frame of the CSC. Let's study the frame and see if any changes should be made.

Before we do a study a few notes should be made. Since we uncoupled the frame, the CSC and the shielding, the stiffness of the frame is now lower. Since only the weight, that is the result of the shielding and the CSC, is acting on the frame (and not the shielding and CSC themselves), the energy and deformation that would be handled by the whole system is now only handled by the frame. Therefore, this is the worse case scenario in terms of deformation and stress of the frame.

The frame is fixed at the feet, where we find the reaction forces, and is affected by forces  $F_1$  to  $F_9$  as well as it's own weight from  $g$ . The frame is made from Aluminium bars ( $\rho = 2770 \text{ kg/m}^3$ ,  $E = 71\,000 \text{ MPa}$  and  $\nu = 0.33$ ) that are held together with structural steel plates.

The bars are modeled as 3D beam elements BEAM188 and the steel plates as shell elements SHELL181, giving us 205687 elements and 264784 nodes. The beam cross-section is the same as the 3D model of the frame.

We can see the deformation results on figure 4.6, where the maximum deformation is 1.4 mm. The forces in the feet are  $R_1 = 5400 \text{ N}$ ,  $R_2 = 5450 \text{ N}$ ,  $R_3 = 8250 \text{ N}$  and  $R_4 = 8270 \text{ N}$ .

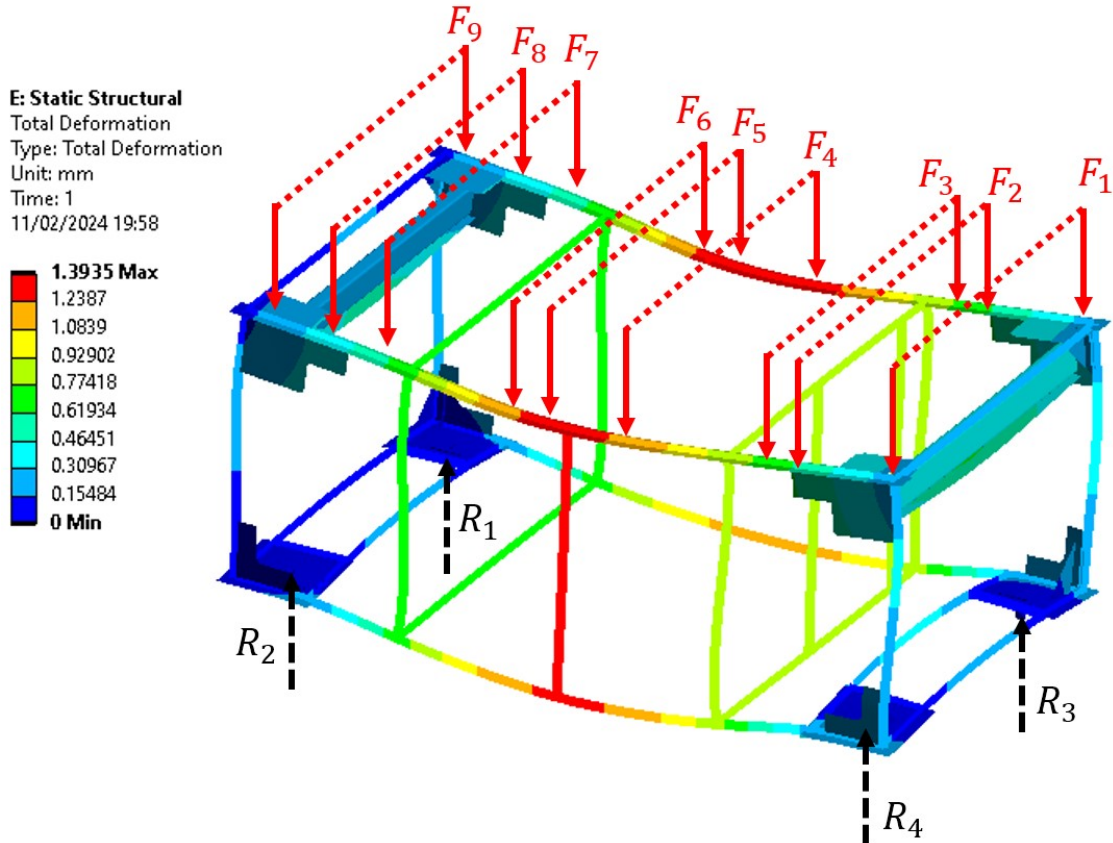


Figure 4.6: Total deformation in the frame and the forces involved.

Looking at the stress in the bars on figure 4.7, we analyse the maximum and minimum combined stress. Maximum combined stress is the combination of axial stress and maximum bending stress, while minimum combined stress is combination of axial stress and minimum bending stress.

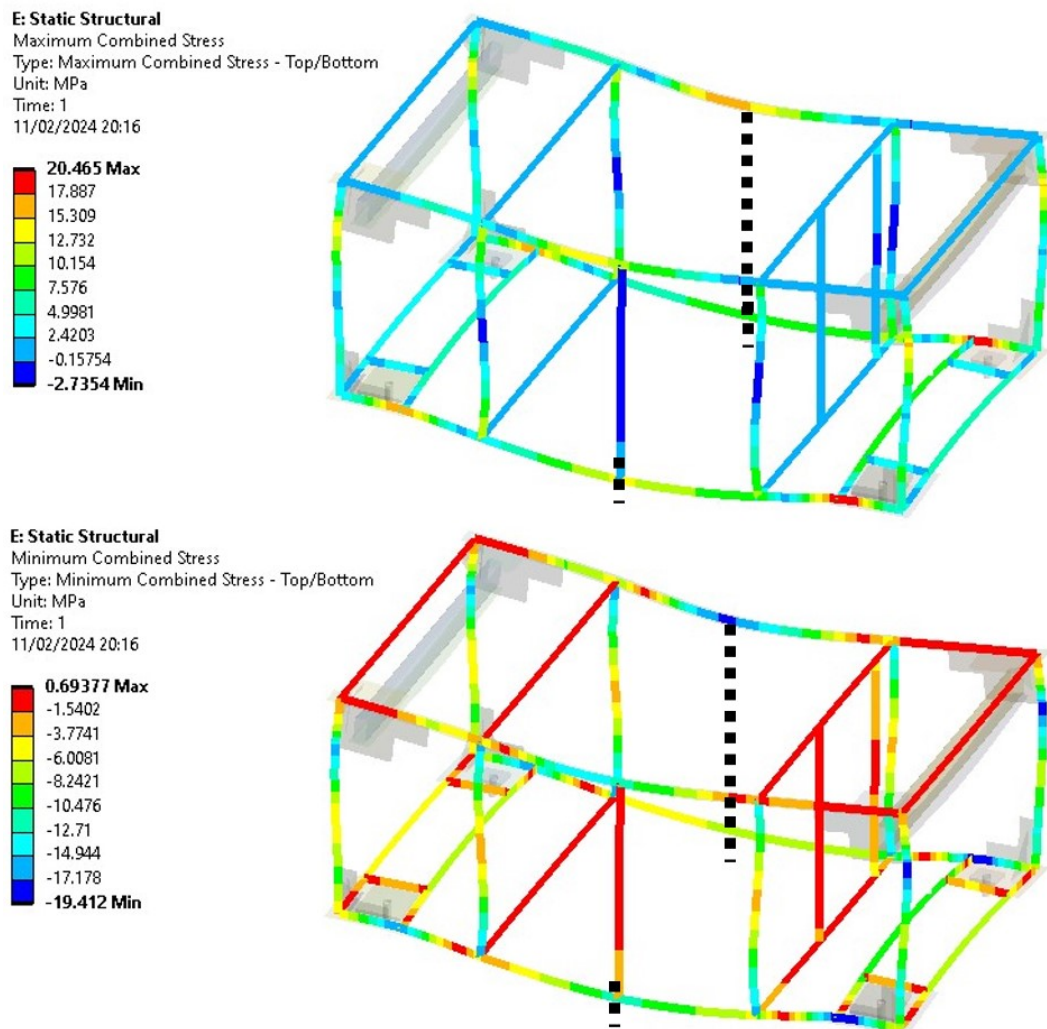


Figure 4.7: Maximum (top) and minimum (bottom) combined stress of the frame.

As we can see the stresses in the bars are significant, as the yield strength of aluminium is 40 MPa and we are at about a 50% threshold. The steel plates have a maximum stress of 100 MPa near the feet.

Recommended action is to add another vertical bar on the right side of the frame, as well as add two more support feet in the middle of the frame (black dashed lines on fig. 4.7).

## 4.3 Cost model

The cost model will give us the first estimation of the price of the shielding, for both the material cost and the manufacturing cost. The upper limit here is 30 000 EUR.

We can make some basic assumptions:

- 3 new brown bar, one is 30 kg; 1 EUR = 1 kg of steel
- 1500 kg of HDPE; 10 EUR = 1 kg of HDPE
- estimated 30h of work; 1 h work = 100 EUR

giving us the estimated price of the shielding at about:

$$3 \times 30 \text{ kg} \times 1 \text{ EUR/kg} + 1500 \text{ kg} \times 10 \text{ EUR/kg} + 30 \text{ h} \times 100 \text{ EUR/h} = 18000 \text{ EUR}. \quad (4.1)$$

We can assume the final price of the shielding will be around 20 000 EUR, not counting the work done by the internal FRS team.

With the models done, we can set the final specification parameters in table 3.2. In the next chapter we will start considering the design of the shielding, based on existing standards.

# 5 Engineering Standards

Since the radiation shielding is responsible for the health of the people working at the FRS, safety is of the highest priority. Therefore, experimental and custom solutions are to be avoided, and standardised well-tested solutions should be prioritised.

While we have the general thicknesses and design of the shielding, specific implementations and design solutions can be found in ISO radiation standards.

Another aspect we must take care of is the fire safety requirements set by GSI.

## 5.1 Radiation standards

The main radiation protection standards we will be looking at are:

- ISO 14152: Neutron radiation protection shielding [3]
- ISO 9404-1: Enclosures for protection against ionizing radiation [4]

### 5.1.1 Ionizing radiation

Ionizing radiation refers to a type of energy released by atoms in the form of electromagnetic waves (gamma or X-rays) or particles (neutrons, electrons, protons). It has enough energy to remove tightly bound electrons from the orbit of an atom, causing the atom to become charged or ionized.

Exposure to ionizing radiation can damage living tissue, leading to skin burns, radiation sickness, and increased risk of cancer. The severity of these effects depends on the dose, which depends on the source strength, distance, and duration of exposure. High doses can cause acute health effects, while lower doses over long periods can increase the risk of long-term health effects.

Focusing specifically on the decay of  $^{252}\text{Cf}$ , we know that it is a significant source of neutrons. These neutrons are a direct product of the fission process, and their high kinetic energy classifies them as fast neutrons. Along with neutrons, gamma radiation is also emitted during the fission process. Neutrons are notoriously difficult to stop, as they do not possess a charge and can therefore only interact with the nucleus of an atom. At the same time, they possess significant mass and energy.

### 5.1.2 Neutron shielding properties

The purpose of neutron shielding is to protect workers and the public from the ionizing radiation produced by neutron sources. Neutron emission is always associated with the production of gamma radiation in fission and fusion and some accelerator-produced reactions. Most neutron interactions within the shielding material also produce gamma radiation.

Shielding should be designed to protect occupationally exposed workers and the general public from neutron and gamma radiation. For slowing down and stopping neutrons it is shown that materials with a high content of hydrogen atoms are very effective. When scattered neutrons collide with hydrogen atoms, they lose energy to the point they are thermalized (they have the same energy as the surrounding material, which depends on the ambient temperature). The remaining energy in the thermal energy range can then be lost through the absorption of the free neutron by the material. Doping the hydrogen-rich material with boron is often used, to give the free neutron an interaction target.

Materials used for the design of neutron radiation protection shielding shall have large cross-sections for neutron moderation and capture. These factors permit the shielding to perform its two primary functions, moderate the energy of the incident neutrons and reduce the neutron fluence. The greater the number of hydrogen atoms present per cubic centimeter, the greater the moderating capability of the material. Particularly suitable are water, polyethylene, polypropylene, paraffin, wood, and concrete.

If we consider other constraints such as weight, workability, solid state at room temperature and price, HDPE is the best candidate. Its properties can be seen in the table below (fig. 5.1).

Designation of material	Description	Relative density	Main contents in $10^{30}$ atoms/m <sup>3</sup>	Additives % of mass	Main mechanical characteristics	Chemical resistance	Ease of decontamination	Maximal allowable temperature	Burning behaviour	Other characteristics
Pure polyethylene type ertalene ®	Pure high density polyethylene, consisting of a polymer ( $\text{CH}_2$ ) chain	0,95	H: $8,18 \times 10^{-2}$ C: $4,08 \times 10^{-2}$	No additives for pure material	Breaking stress (traction): 42 MPa (compression): not available	Moderate resistance to acids, oxidizing agents and solvents	Depends on the surface condition	80 °C	Burnable material	Available in slabs and easily workable. Very high fire load. Medium resistance to radiation. It can be charged with fire proofing elements and protected by a casing.

Figure 5.1: Table of properties of HDPE [3].

The main issue this material has is its lack of fire resistance. However, there exist options on the market that contain the proper additives to improve fire performance.

### 5.1.3 Radiation shielding design principles

With the material selected, we can focus on finding a design solution for the shielding. Those can be found in ISO 9404-1 [4]. Any mechanical way to attach and bond the shielding with fasteners is out of the question, as drilling the shielding would present a gap. Our basic design also has a big flaw, as rectangular blocks can show small gaps where they are put together. Both the issue of fastening the shielding blocks, as well as eliminating the gaps, can be solved by using a chevron design on the building blocks of the shielding (fig. 5.2).

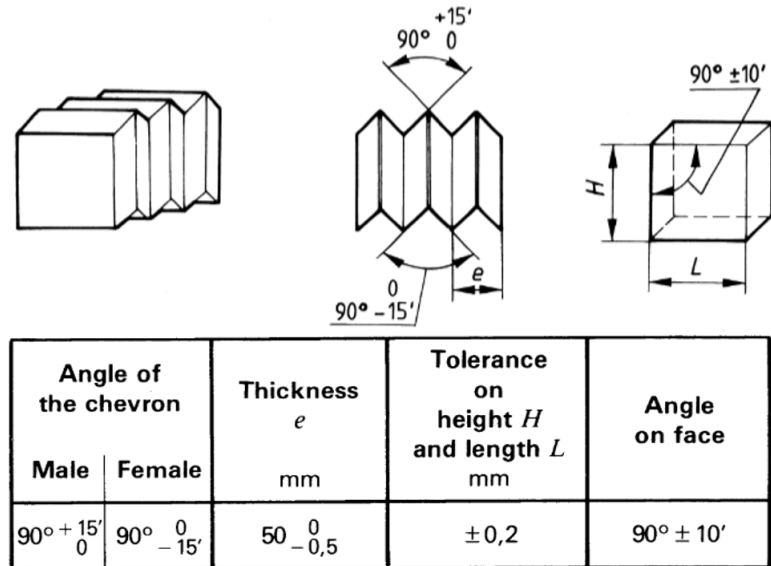


Figure 5.2: Example of a three-chevron brick [4].

The way the blocks interlock with each other ensures they are structurally stable (fig. 5.3). And since the parting lines between different blocks zigzag in the direction of the neutron particle path, no particle will ever find a gap without shielding.

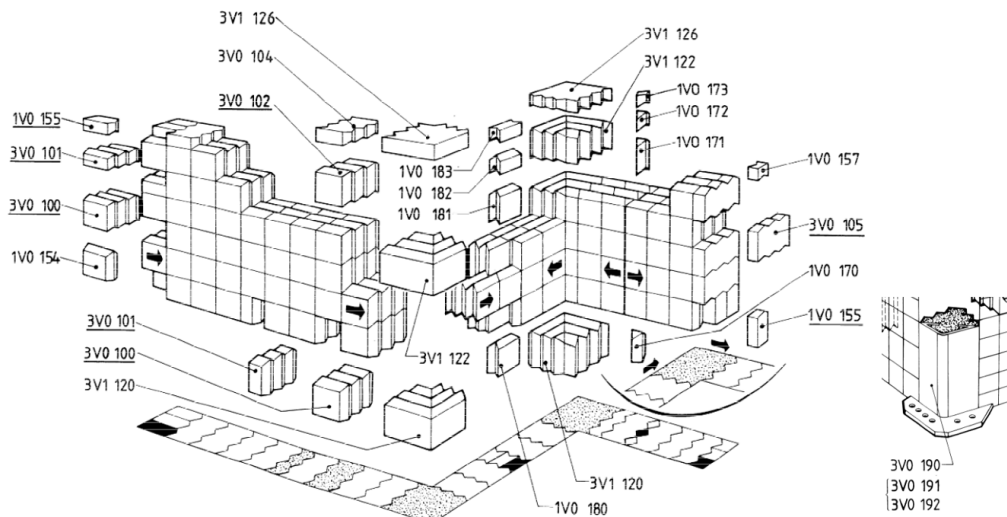


Figure 5.3: General diagram of a chevron block assembly [4].

## 5.2 Fire safety standards

Neutron shielding material must be able to withstand the environmental temperatures associated with its location as well as any heat induced while performing its design function. It should be fire resistant, not overheat, and keep its mechanical properties stable during normal working operations.

### 5.2.1 Conditions of operation of the CSC experiment

The experiment will be performed under the following conditions, from a fire safety perspective:

- The inside compartment is heated up to 130 °C. There is a vacuum between the inside and outside shell. The inside shell is at least 5 cm away from the outside one.
- The shielding doesn't cover the top part. It is open.
- During the experiment the cave is closed. But the roof will be opened. It can also be closed if needed.
- 1500 litres of flammable material is used (cca. 1500 kg of PE)

### 5.2.2 Fire classification of construction products and elements

GSI uses DIN EN 13501-1 or DIN 4102-1 as its internal fire safety standards. We will focus only on the first one [5].

For a material to be classified under DIN EN 13501-1, the following steps are needed:

1. Classify if the material is a general construction product, used as a flooring product, or used as a pipe thermal insulation product. For the following study, we will exclude floorings or pipe insulation.
2. Reactions to different fire tests are needed:
  - EN 13823 Exposure to thermal attacks,
  - EN 1182 Non-combustibility test,
  - EN ISO 1716:2010 Determination of the gross heat of combustion,
  - EN ISO 11925-2 Ignitability of products subjected to direct impingement of flame - Single-flame source test.
3. From those tests, are series of metrics are obtained (fig. 5.4)

Performance levels for each specific parameter are determined from the test methods.

a) Continuous parameters

EN ISO 1182	$\Delta T$
	$\Delta m$
	$t_f$
EN ISO 1716	<i>PCS</i> and possibly <i>PCI</i>
EN 13823	$FIGRA_{0,2MJ}$ and $FIGRA_{0,4MJ}$
	$THR_{600s}$
	<i>SMOGRA</i>
	$TSP_{600s}$

The mean value ( $m$ ) shall be determined for the performance level for each parameter. The classification shall then be determined from this value as described in 7.3.

b) compliance parameters

EN 13823	<i>LFS</i> and flaming droplets/particles
EN ISO 11925-2	$F_s$ and flaming droplets/particles

The individual results for each parameter shall be assessed to determine the classification as described in 7.4.

$\Delta T$	temperature rise [K]
$\Delta m$	mass loss [%]
$F_s$	flame spread [mm]
<i>FIGRA</i>	fire growth rate index used for classification purposes (Fire growth rate)
$FIGRA_{0,2MJ}$	fire growth rate index at <i>THR</i> threshold of 0,2 MJ
$FIGRA_{0,4MJ}$	fire growth rate index at <i>THR</i> threshold of 0,4 MJ
<i>LFS</i>	lateral flame spread [m]
<i>PCS</i>	gross calorific potential [MJ/kg or MJ/m <sup>2</sup> ] (Gross calorific potential)
<i>PCI</i>	net calorific potential [MJ/kg or MJ/m <sup>2</sup> ]
<i>SMOGRA</i>	smoke growth rate
$t_f$	duration of sustained flaming [s] (duration of flaming)
$THR_{600s}$	total heat release within 600 s [MJ]
$TSP_{600s}$	total smoke production within 600 s [m <sup>2</sup> ]
$m'$	mean value of the set of results of a continuous parameter determined in accordance with the relevant test method using the minimum number of tests as specified in the test method
$m$	mean value of the set of results of a continuous parameter determined in accordance with the procedure in 7.3 and used for classification

Figure 5.4: Fire test according to ISO 13501-1 [5]

The metrics in fig. 5.4 are used to classify the material into a category:

- **Classes E, F:** A product applying for class E or F shall be tested in accordance with EN ISO 11925-2 with 15 s exposure time. To reach class E, there shall be no flame spread in excess of or equal to 150 mm vertically from the point of application of the test flame within 20 s from the time of application.
- **Classes D, C, B:** A product applying for class D, C or B shall be tested in accordance with EN ISO 11925-2 with 30 s exposure time. There shall be no vertical flame spread in excess of or equal to 150 mm from the point of application of the test flame within 60 s from the time of application. Products satisfying the EN ISO 11925-2 criteria for class D, C or B shall additionally be tested in accordance with EN 13823. FIGRA<sub>0,2MJ</sub> shall first be used to determine whether the requirement for Class A2 or B is met and FIGRA<sub>0,4 MJ</sub> shall be used to determine whether Class C or D is met.
  - D: FIGRA<sub>0,4 MJ</sub> ≤ 750 W/s
  - C: No lateral flame at edge, FIGRA<sub>0,4 MJ</sub> ≤ 250 W/s , THR<sub>600s</sub> ≤ 15 MJ
  - B: No lateral flame at edge, FIGRA<sub>0,2 MJ</sub> ≤ 120 W/s , THR<sub>600s</sub> ≤ 7,5 MJ
- **Class A2:** A product applying for class A2 shall be tested in accordance with EN ISO 1182 and EN ISO 1716. If the product is a composite, individual components are tested individually. Additionally, all products applying for class A2 shall be tested in accordance with EN 13823 and must pass the criteria for class B.
  - a) EN ISO 1716: PCS ≤ 3,0 MJ/kg (4,0 MJ/kg for external component)
  - b) EN ISO 1182 : ΔT ≤ 50°C and Δm ≤ 50% and  $t_f \leq 20$  s
- **Class A1:** A product applying for class A1 shall be tested in accordance with EN ISO 1182 and EN ISO 1716. If the product is a composite, individual components are tested individually. Additionally, all products applying for class A2 shall be tested in accordance with EN 13823.
  - a) EN ISO 1716: PCS ≤ 2,0 MJ/kg or PCS ≤ 2,0 MJ/m<sup>2</sup>
  - b) EN ISO 1182 : ΔT ≤ 30°C and Δm ≤ 50% and  $t_f = 0$  s
  - c) EN 13823: FIGRA<sub>0,2MJ</sub> ≤ 20 W/s and LFS < edge of specimen
  - d) EN 13823: THR<sub>600s</sub> ≤ 4,0 MJ and s1, d0

Classifications for smoke production s1, s2 and s3 are deduced from the measuring data obtained from testing in accordance with EN 13823.

- s1: SMOGRA ≤ 30 m<sup>2</sup>/s<sup>2</sup> and TSP<sub>600s</sub> ≤ 50 m<sup>2</sup>.
- s2: SMOGRA ≤ 180 m<sup>2</sup>/s<sup>2</sup> and TSP<sub>600s</sub> ≤ 200 m<sup>2</sup>.
- s3: Products which do not comply with the s1 and s2 criteria.

Classifications d0, d1 and d2 for flaming droplets are deduced from observations of flaming droplets and particles with EN 13823:

- d0, if no flaming droplets/particles occur within 600 s when tested
- d1, if no flaming droplets/particles, persisting longer than 10 s, occur within 600 s when tested
- d2 if no performance is declared, or if the product does not comply with the d0 and d1

Example classes that can be assigned: A2-s1-d0, B-s3-d0, C-s3-d1, ...

### 5.2.3 UL94 V Flammability Standard

In the later section, we didn't have the necessary ISO 13501-1 categorisation available for the specific materials we were looking into. We also studied other standards, like DIN EN 45545-1: Fire protection for railway vehicles [6]. The only standard we will go into some more detail is UL94 [7] for a material in section 6.2.3. The material's company used a different fire standard, which we will explain here and later use as a comparison to see where within the GSI fire standard the material would fit.

The UL94 standard [7] for a material is done the following way. A total of 10 specimens (2 sets) are tested per thickness. Five specimens of each thickness are tested after conditioning for 48 hours at 23 °C and 50% relative humidity. Five specimens of each thickness are tested after conditioning for 7 days at 70 °C. Each specimen is mounted with long axis vertical. Each specimen is supported such that its lower end is 10 mm above Bunsen burner tube. A blue 20 mm high flame is applied to the centre of the lower edge of the specimen for 10 seconds and removed. If burning ceases within 30 seconds, the flame is reapplied for an additional 10 seconds. If the specimen drips, particles are allowed to fall onto a layer of dry absorbent surgical cotton placed 300 mm below the specimen. The test scheme can be seen on figure 5.5.

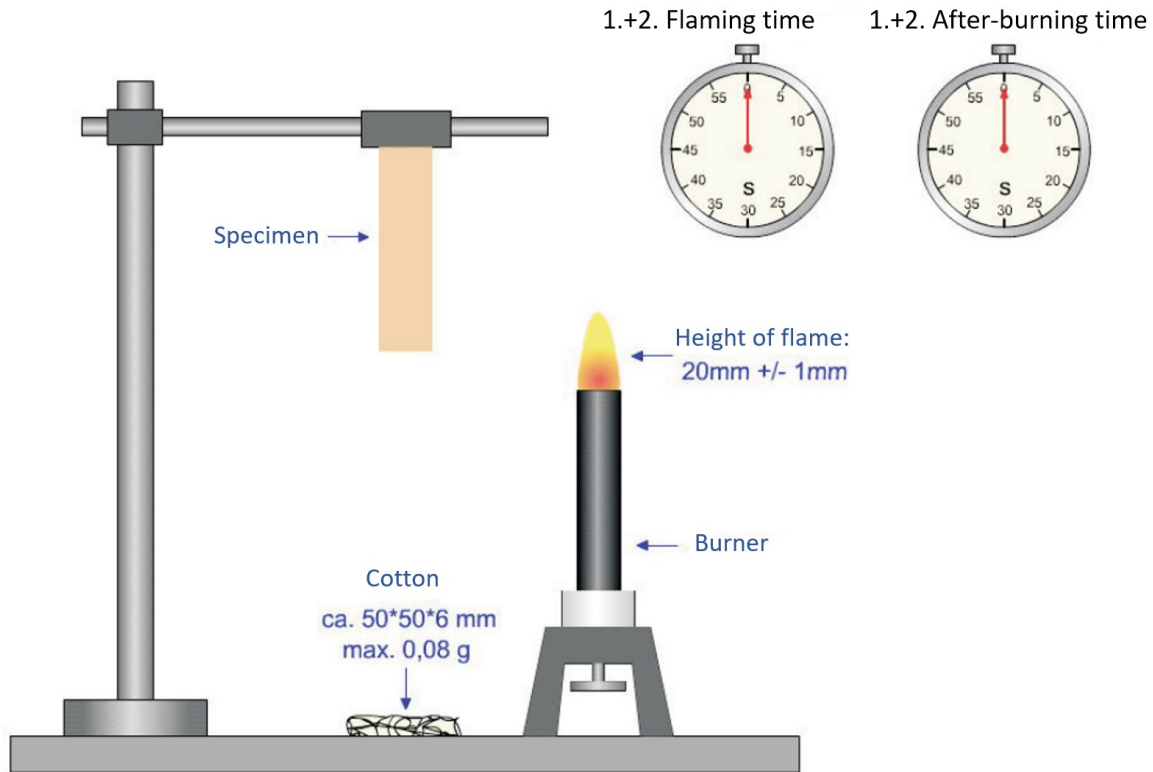


Figure 5.5: UL94 burning test [7].

We will now look at the process of finding the specific shielding material and the companies that produce them.

# 6 Material and company selection

In the previous chapters, we discussed the required properties of the material used in the shielding. The high hydrogen content of HDPE allows good neutron shielding attenuation. On the other hand, polyethylene is known to be a combustible material once ignition temperature is reached. Therefore we had to find either an alternative or find a way to make HDPE work within the fire safety regulations of GSI.

## 6.1 The selection process

The selection process for the shielding material was the lengthiest and most difficult part of the project. Not only does actual material on the market differ from pure polyethylene found in the literature [3], but we also had to consider manufacturability (producible dimensions of basic plates) the company demands, costs, etc. In the following section, we will go through the iterative process of material selection.

The first material option, the material option we started with and that the simulation was done with, was the generic, pure HDPE. As seen in fig. 5.1. According to ISO DIN EN 13501-1 such a material is a fire hazard, as it has a high fire load. We wanted to preserve the simulation validity, so the only way to use pure HDPE would be to encase it into steel, which then protects the material against direct fire exposure.

Steel-encased HDPE shielding is a known solution and is used at other sites at GSI. There were also some HDPE steel-encased blocks readily available at GSI, so we considered integrating them into our design. We quickly ran into two problems:

1. Steel sheets are not adequate shielding material for neutron attenuation, as the nuclear cross-section of iron atoms isn't sufficiently large for neutron-nucleus interaction. Where two steel-plated HDPE blocks would meet is a weak point in the shielding. The available blocks only had basic rectangular shapes, so no chevron interlocking was available and the shielding is compromised.
2. The variety in the size of steel-plated blocks was not large enough to integrate into the limited space available around the CSC.

So in any case we would have to encase custom-sized and shaped HDPE blocks into steel to make the design viable.

Here we considered exchanging HDPE with paraffin wax since it's commonly used for radiation neutron shielding too. Another benefit is also that it has the consistency of wax at room temperature, which would make it easier to use with steel casing, as it could simply be poured inside. Since the radiation simulation was done for HDPE, let's make a closer comparison between it and paraffin [3].

Paraffin wax typically contains about 13-14% hydrogen by weight and has a density of around 900 kg/m<sup>3</sup>. HDPE has an H-content of 14-15% and a density of around 950 kg/m<sup>3</sup>. Polyethylene is denser and has a higher H-content making it more efficient at radiation attenuation. A thicker shielding would be needed if wax is used. From a fire safety perspective, paraffin wax has a relatively low melting point, typically between 46°C and 68°C. It is flammable and can ignite easily when exposed to an open flame or high temperatures. The ignition temperature of polyethylene is higher than that of paraffin wax. It typically ignites at temperatures above 300°C, which is significantly higher than the melting point of paraffin wax. The price of paraffin is comparable to polyethylene and is therefore not a factor.

Apart from easier use with a metal shell, paraffin wax has few benefits. So here we refocused on Polyethylene and researched into special grade fire resistant HDPEs and one of them is what we chose.

## 6.2 Companies contacted for fire-resistant HDPE

### 6.2.1 Röchling Group

Röchling Group is a German-based company that offers high-performance materials specifically developed for neutron shielding made of thermoplastics, laminated densified wood, and glass fiber-reinforced material. These materials have different hydrogen contents for decelerating fast neutrons, are available with boron or lithium additives depending on the shielding material used, and are suitable for a wide range of continuous operating temperatures.

The commercial material *Polystone® M nuclear* (Polyethylene: PE-UHMW) has additives that give PE fire-resistant properties. The company never replied, so we moved forward with the selection process.

### 6.2.2 JCS Nuclear Solutions

JCS is a US company with distribution available in Europe. JCS offers an extensive selection of radiation shielding for neutron, gamma, and X-ray fields. These materials can be supplied in sheets, rods, pellets, flexible sheets, and even pre-molded to specifications. They also offer machining which is one of the requirements. Especially interesting for us is their *JC207HD Self-Extinguishing Borated Polyethylene®*. While they didn't have the exact fire-safety standard GSI requires, the properties list was detailed enough to do a comparison. The material would be a good fit, but the added boron is not a requirement and it adds to the price. Apart from that it's not a company in Germany which makes it more difficult to order from.

### 6.2.3 Mitsubishi Chemical Group

The final company, and the company we selected, was Mitsubishi Chemical Group. The Mitsubishi Chemical Group is a leading global manufacturer and supplier of chemicals, performance products, and materials. It is part of the Mitsubishi Group, which is a conglomerate of independent Japanese multinational companies covering a range of businesses which share the Mitsubishi brand, trademark, and legacy.

The Mitsubishi Chemical Group operates across multiple sectors, including performance products, industrial materials, and health care. Its product line includes a wide variety of chemicals, plastics, and materials used in various industries such as automotive, electronics, construction, pharmaceuticals as well as the radiation protections sector. The company is known for its commitment to sustainability, innovation, and the development of advanced materials and solutions that contribute to addressing global environmental and societal challenges. They also have a German base in Dusseldorf and they have worked with Jülich on a shielding project in the past.

We initially contacted them regarding their *TIVAR® BurnGuard UHMW-PE*, which is a static dissipative and flame retardant material specifically developed to improve the flammability behavior of unfilled polyethylene grades. This grade in particular possesses a UL94 V-0 Flammability Rating [7]. Due to these characteristics, BurnGuard excels in applications where key components may be exposed to combustion.

We were able to have multiple meeting with company representatives, where we discussed the design requirements to make the plates manufacturable, the price and the lead-time, which is 8 to 10 weeks. We discovered the price varies depends on the thickness of the ordered plates. In summary:

- the width of the plates can be a max. of 2.4 m and with a length of 6 m;
- the thickness of the plates can be between 11.5 mm to 120 mm;
- the best price/kg are the 50 mm plate (8 EUR/kg) and 100 mm plate (9.5 EUR/kg);
- the thickness tolerance is  $\pm 0.4$  mm;
- they can't produce the steel holsters to hold the shielding up and
- the chevron design (fig. 5.2) has to be adapted to manufacturability (fig. 6.1).

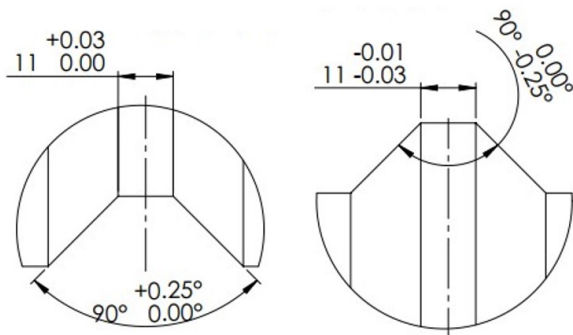


Figure 6.1: Chevron design changed by Mitsubishi.

### 6.2.3.1 The change in radiation dose

The last thing we have to check is if BurnGuard has radiation attenuation properties similar to pure polyethylene with which the radiation simulation was done. We can look at the density of hydrogen atoms in BurnGuard PE compared to a regular PE. Their ratio will show how much thicker the new shielding has to be. If we assume linear dependence between the dose and thickness of the shielding, then this ratio will also show how much higher the dose rate will be if you keep the thickness unchanged.

We started with normal HDPE with properties visible on figure 5.1. We can see  $8.18 \times 10^{-2}$  hydrogen atoms per  $10^{30}$  atoms that are located in one  $\text{m}^3$ . That equates to  $8.18 \times 10^{22}/\text{cm}^3$  hydrogen atoms. For the given density of  $0.96 \text{ g/cm}^3$  that is 14-15% hydrogen content (the molar mass of hydrogen is  $1.00784 \text{ g/mol}$ ).

If we want to use BurnGuard HDPE, the hydrogen weight content is 11% according to Mitsubishi. We can calculate the hydrogen amount per  $\text{cm}^3$ :

$$H [\text{cm}^3] = H\% \cdot \rho \cdot \frac{\text{mol}}{M(H)} \cdot N_A$$

$$H [\text{cm}^3] = 11\% \cdot 1.01 \text{ g/cm}^3 \cdot \frac{\text{mol}}{1,00784 \text{ g/mol}} \cdot 6,022 \cdot 10^{23} \text{ mol}^{-1}$$

$$H [\text{cm}^3] = 6,63 \times 10^{22}/\text{cm}^3.$$

The material has  $6,63 \times 10^{22}/\text{cm}^3$  of hydrogen atoms. If we compare BurnGuard to the original simulation with pure PE, we see we have a factor of 1,23 dose increase. This would mean an increase in the thickness of the shielding is needed.

But after a discussion with the FRS team, and taking into account the reason for a lower hydrogen percentage in BurnGuard compared to pure PE, is that BurnGuard has other additives. Those additives also contribute to neutron attenuation, therefore we will not be re-running any simulation or changing the current design and thickness.

With the fully completed specification list, selected material company and knowing any design limitation and recommendations from the company and the engineering standards, we can proceed to the design stage of the shielding.

# 7 Design process

The main bulk of work in the internship went towards the iterative design of the radiation shielding mechanical solution. We started with simple concept sketching that was later developed into a full CAD design on which the drawing are based.

## 7.1 Mechanical solution conceptualisation

Here we used brainstorming techniques to find design options and alternatives for the shielding, where creative thinking was encouraged (fig. 7.1). Here the specifications were kept in mind, but not enforced.

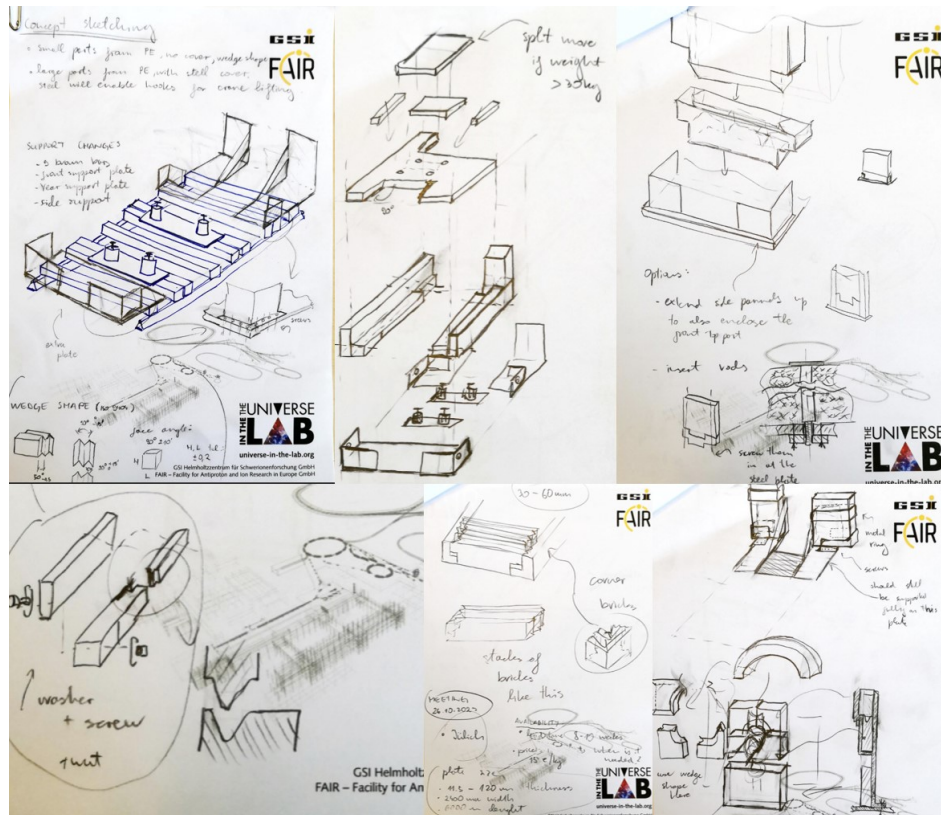


Figure 7.1: Concept sketching for the stopping cell shielding.

## 7.2 The iterative process and the final design

Once the concepts were thought of, they went through polishing in which the specifications were accounted for. We will show a final shielding solution on fig. 7.2 and the installed glovebox design on 7.3.

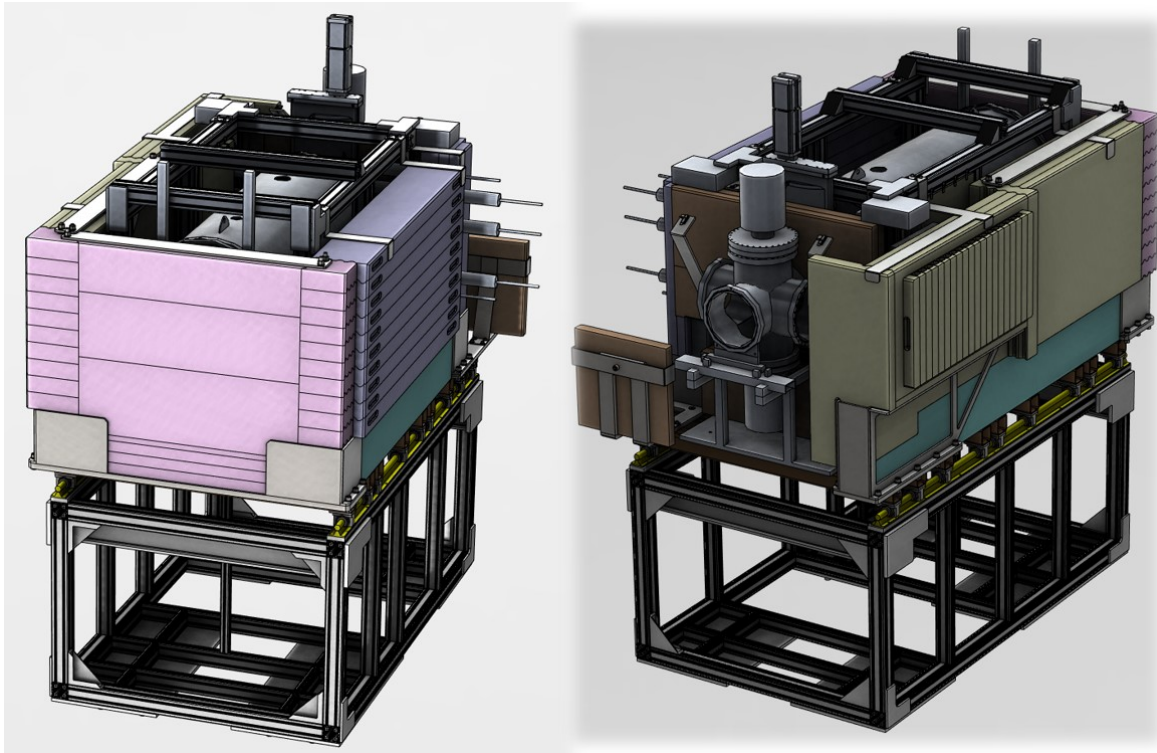


Figure 7.2: Full shielding solution from the front (left) and the rear (right).

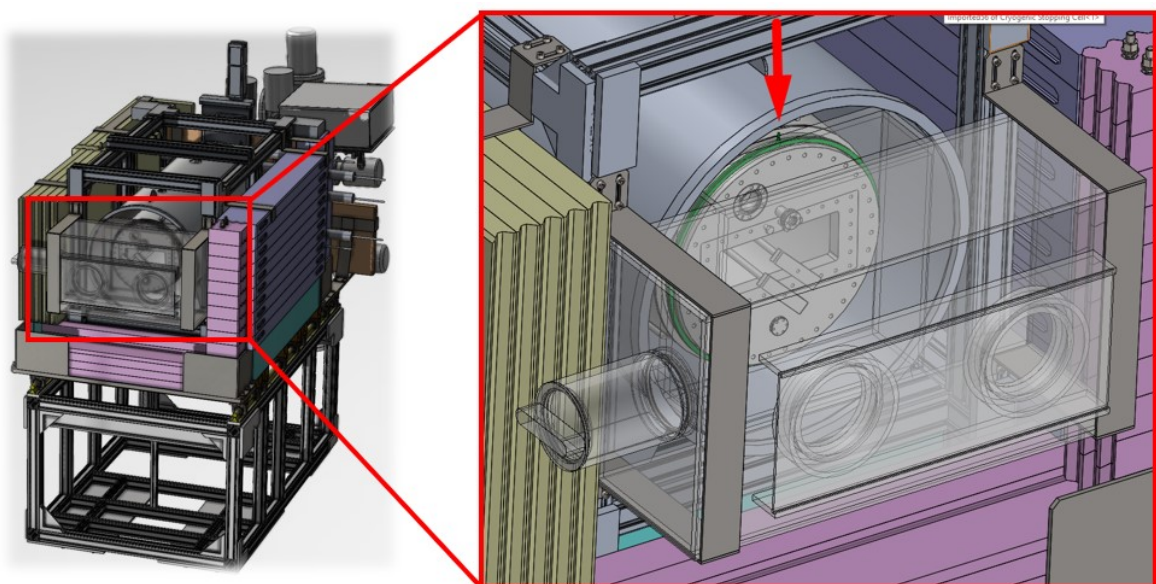


Figure 7.3: Installed glovebox within the shielding.

To see the individual components we can take the first page out of the technical documentation. We can see the exploded view of the shielding assembly on fig. 7.4. We incorporate many steel pieces that serve as fixtures and holders for the shielding. The shielding itself is fully made from 50 and 100 mm BurnGuard plates. Some have the proposed chevron design that help with both radiation shielding as well as structural stability.

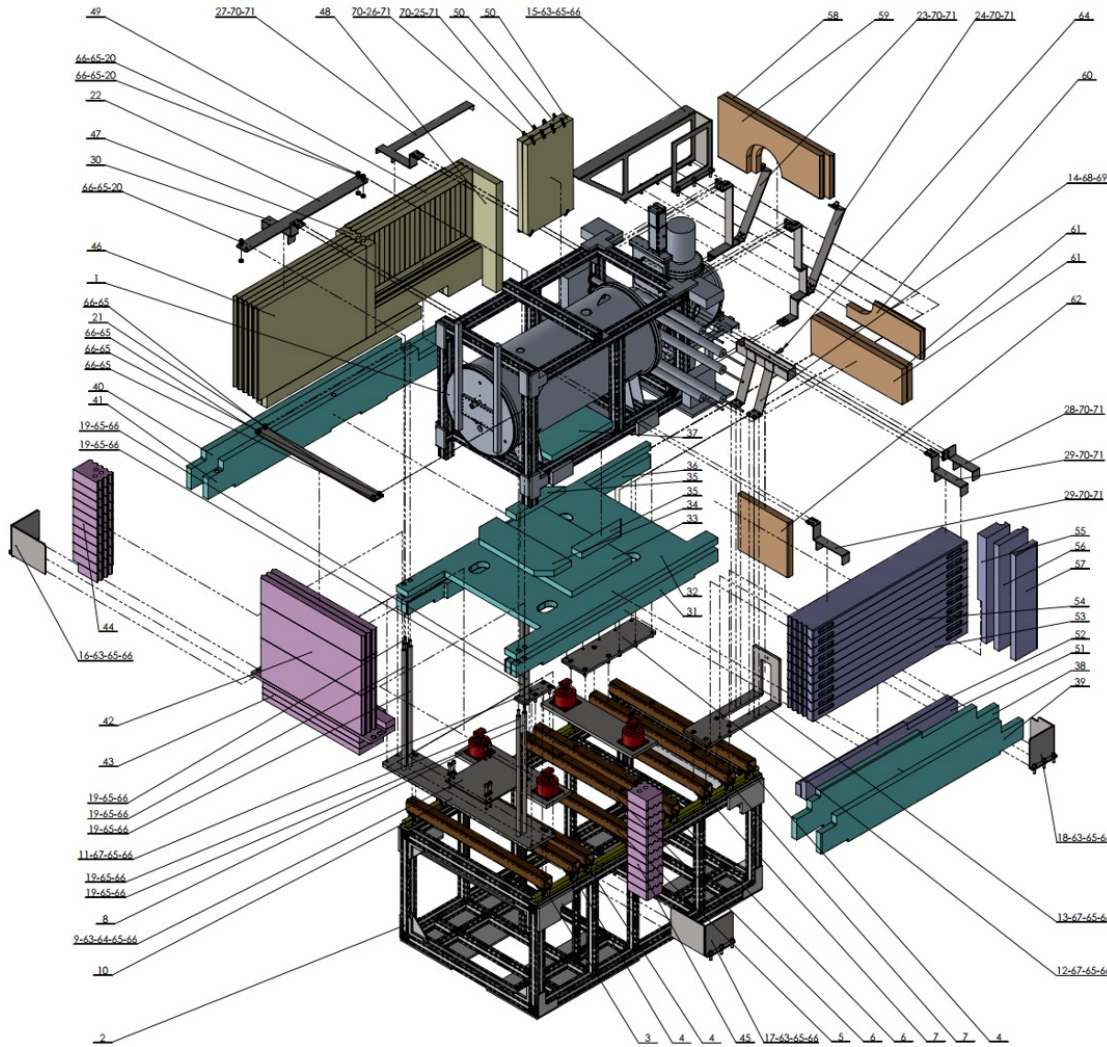


Figure 7.4: Exploded view of the shielding.

### 7.3 Technical documentation

As part of the documentation to be used during the manufacturing process of the HDPE parts (done at Mitsubishi) as well as steel components (GSI), we made:

- a 100 page assembly document with individual part dimensions and specifications;
- a step-by-step assembly instruction manual.

Those documents are found in the appendix.

## 8 Conclusion

This internship report has meticulously detailed the process of designing, simulating, and selecting materials for the radiation shielding of the FRS Ion Catcher, highlighting the significant intersection of theory, practical engineering, and safety standards. The internship journey encapsulated the challenge of balancing neutron shielding effectiveness with material properties, cost considerations, and fire safety standards, culminating in a practical solution that will be in use by the end of 2024. The successful selection and design of HDPE-based shielding, complemented by the innovative chevron block assembly for gap minimization successfully addressed complex radiation safety requirements.

This work not only contributes to the safety and efficiency of the FRS Ion Catcher but could also be used for future endeavors in the field of radiation shielding design for experiments involving ionizing radiation, emphasizing the importance of interdisciplinary collaboration, rigorous standards adherence, and creative problem-solving.

## 9 Bibliography

- [1] Y. Waschitz, D. Amanbayev, A. Spătaru, I. Mardor, T. Dickel, E. Cohen, O. Aviv, S. A. San Andrés, D. Balabanski, S. Beck, *et al.*, “Independent isotopic fission yields of  $^{252}\text{cf}$  spontaneous fission via mass measurements at the frs ion catcher,” in *EPJ Web of Conferences*, vol. 284, EDP Sciences, 2023.
- [2] W. Plaß, T. Dickel, S. Purushothaman, P. Dendooven, H. Geissel, J. Ebert, E. Haettner, C. Jesch, M. Ranjan, M. Reiter, *et al.*, “The frs ion catcher—a facility for high-precision experiments with stopped projectile and fission fragments,” *Nuclear Instruments and Methods in Physics Research Section B: Beam Interactions with Materials and Atoms*, vol. 317, pp. 457–462, 2013.
- [3] “Neutron radiation protection shielding — design principles and considerations for the choice of appropriate materials,” standard, International Organization for Standardization, Geneva, CH, Mar. 2001.
- [4] “Enclosures for protection against ionizing radiation - lead shielding units for 150 mm, 200 mm and 250 mm thick walls,” standard, International Organization for Standardization, Geneva, CH, Mar. 1991.
- [5] “Fire classification of construction products and building elements - part 1: Classification using data from reaction to fire tests,” standard, International Organization for Standardization, Geneva, CH, Aug. 2017.
- [6] “Fire protection on railway vehicles - part 1: General,” standard, CEN-CENELEC, DE, Mar. 2013.
- [7] “UL94 brandklassifikationstests für kunststoff - materialien,” standard, Appra Gruppe, Daun, DE, Aug.

# **10 Appendix**

The appendix consists of:

1. A 100 page assembly document with individual part dimensions.
2. A step-by-step assembly instruction manual.
3. Project timeline on a week-by week basis.